Sensors and Materials, Vol. 38, No. 5 (2026) 2621–2632
MYU Tokyo

S & M 4458

1D Convolutional Neural Network-based Fault Diagnosis Technique for Power Capacitors Using Time-domain Electrical Signals

Hong-Wei Sian, Meng-Hui Wang,* and Chen-Hsiang Sun

Department of Electrical Engineering, National Chin-Yi University of Technology,
No. 57, Sec. 2, Zhongshan Rd., Taiping Dist., Taichung 411030, Taiwan (R.O.C.)

(Received December 12, 2025; accepted March 16, 2026)

Keywords: power capacitor, time domain, 1D convolutional neural network, fault diagnosis, distribution system

Power capacitors are essential reactive power compensation devices in distribution systems, improving power factor, enhancing voltage quality, and reducing feeder losses. However, factors such as internal defects, poor connections, and overload operation can lead to insulation degradation and capacitance deterioration. In this study, we propose a fault detection method based on a 1D convolutional neural network that directly classifies capacitor conditions using time-domain charging harmonic current signals without the need for additional feature extraction. Low-voltage charging harmonic currents were generated using a power testing system, and high-frequency current sensors together with an oscilloscope were employed to acquire the waveform data. The developed model effectively learns the intrinsic characteristics of the current signals and accurately identifies capacitor operating states. Experimental results showed that the proposed method achieves a degradation-fault detection accuracy of 97.78%, demonstrating its effectiveness and practical value for the condition monitoring and preventive maintenance of power capacitors.

1. Introduction

Power capacitors are essential components in distribution networks for reactive power compensation, contributing to power factor regulation, voltage stabilization, and feeder loss reduction. During long-term operation or under adverse conditions such as overvoltage stress, harmonic distortion, improper wiring, or mechanical damage, the metallized film and dielectric materials within capacitors may gradually degrade. This degradation can lead to capacitance reduction or insulation failure, adversely affecting system reliability and increasing maintenance costs. Therefore, the development of automated and reliable diagnostic techniques for capacitor degradation and failure is of increasing importance in modern distribution systems.[1–3]

In recent years, deep learning has been widely applied to power system signal analysis and equipment fault diagnosis. The convolutional neural network (CNN) and its variants have demonstrated strong feature representation capabilities in both time-domain and frequency-

*Corresponding author: e-mail: wangmh@ncut.edu.tw
https://doi.org/10.18494/SAM6121

ISSN 0914-4935
https://myukk.org/

domain applications, including partial discharge analysis and waveform classification.[4–7] More recent studies have indicated that the 1D convolutional neural network (1D-CNN) is particularly suitable for directly processing raw electrical time-series signals without requiring image transformation or handcrafted feature extraction, enabling efficient end-to-end learning with high diagnostic accuracy.[8–10]

Despite these advances, capacitor degradation diagnosis remains challenging. The measured current signals associated with capacitor degradation typically exhibit low amplitudes and are susceptible to high-frequency noise, which can result in information loss when conventional frequency-domain or feature-based approaches are applied.[11,12] Moreover, the differences among various degradation levels are often subtle, requiring models capable of identifying weak and localized signal variations. From a practical perspective, diagnostic methods must also consider deployment feasibility, including inference latency and front-end sensing requirements. Recent research suggests that integrating high-frequency current transformers (HFCTs) with time-domain deep learning models can enhance detection sensitivity while reducing reliance on complex signal preprocessing.[13,14]

Motivated by these considerations, in this study, we propose a 1D-CNN-based diagnostic framework for power capacitor degradation and failure assessment. High-frequency charging harmonic currents are acquired using an HFCT during low-voltage charging tests and conditioned through a dedicated high-pass filtering and amplification circuit. The resulting time-domain waveforms are directly fed into the 1D-CNN for end-to-end classification. Six capacitor conditions (normal, 20, 40, 60, and 80% degradation, and failure) are constructed using retired capacitor samples to validate the proposed method. The diagnostic performance and inference efficiency are further compared with those of a 2D-CNN and an extension neural network (ENN), demonstrating the superior accuracy and computational efficiency of the proposed approach. The remainder of this paper presents the construction of the degradation models, the measurement and front-end circuit design, the architecture and training details of the 1D-CNN, and a comprehensive discussion of the experimental results.

2. Proposed Fault Diagnosis Algorithm

In this study, we propose a fault diagnosis method for power capacitors based on a 1D-CNN, which directly analyzes high-frequency time-domain charging harmonic current signals. CNNs are widely used supervised deep-learning architectures and can be categorized into 1D, 2D, and 3D models according to the dimensionality of the convolution operation. Specifically, 1D-CNNs are well suited for processing time-series or linear signal data,[15,16] 2D-CNNs are typically used for image classification,[17,18] and 3D-CNNs are predominantly applied to volumetric medical imaging and video analysis.[19,20] Given that the measured charging harmonic currents in this study are high-frequency time-domain signals, a 1D-CNN is more appropriate for capturing their local temporal features and is therefore adopted as the core analytical architecture. The model employs multiple convolution, activation, and pooling layers to automatically extract salient features, followed by fully connected layers that integrate these representations to classify the fault conditions of power capacitors.

2.1 Convolution layer

In a 1D-CNN architecture, convolutional layers are responsible for extracting local structural features from time-series data. A convolution kernel slides along the temporal axis to capture localized signal variations, such as transient spikes, slope changes, and specific frequency components. Let the input sequence be denoted as $x(i)$ and the kernel length be k; the one-dimensional convolution operation can then be expressed as

$$y(i) = \sum_{t=0}^{k-1} x(i+t) \otimes w(t) + b \,. \tag{1}$$

In this formulation, $x(i)$ denotes the input signal value at time index i, $w(t)$ represents the convolution kernel of length k, b is the bias term, ⊗ indicates the convolution operation, and $y(i)$ is the resulting convolution feature at position i. By employing multiple convolution kernels, the network can simultaneously capture features associated with different temporal scales and frequency components. Following the convolution operation, a nonlinear activation function is applied to enhance the model's representational capacity. In this study, we adopted the Rectified Linear Unit (ReLU), defined as

$$f(z) = \max(0, z) \,. \tag{2}$$

In this formulation, z represents the convolution output. The ReLU activation function provides computational efficiency, stable gradient propagation, and faster convergence, enabling the effective preservation of salient signal features while mitigating gradient-vanishing issues. These characteristics make ReLU well suited for deep-learning applications involving time-domain electrical signals.(21,22)

2.2 Pooling layer

After convolution and activation operations, the extracted feature maps are typically passed to a pooling layer for downsampling. This process condenses salient features, reduces data dimensionality, decreases computational cost, and enhances robustness against temporal shifts and local signal fluctuations. Common pooling strategies include max pooling and average pooling. Max pooling is particularly suitable for the high-frequency time-domain electrical signals examined in this study because of its effectiveness in capturing transient spikes and peak characteristics. The max-pooling operation can be expressed as

$$p(i) = \max_{m \in R} y(i+m) \,. \tag{3}$$

In this operation, $y(i)$ denotes the feature value before pooling and R represents the pooling region. The max-pooling layer selects the largest value within each pooling window as the representative feature, thereby preserving the most discriminative local responses of the signal. By applying this downsampling mechanism, the model reduces the length of the feature maps, mitigates the risk of overfitting, and enhances computational efficiency and stability during both training and inference.

2.3 Fully connected layer

After multiple convolution and pooling operations, the high-dimensional features extracted by the network are flattened into a 1D vector and fed into the fully connected layer to establish a mapping between the features and output classes. Let the flattened feature vector be $h = [h_1, h_2, ..., h_n]$; then, the linear combination for the k-th output of the fully connected layer can be expressed as

$$z_k = \sum_{\{i=1\}}^{n} h_i W_{ik} + b_k \,. \tag{4}$$

Here, W_{ik} denotes the weight coefficient, b_k is the bias term, and z_k represents the output score for the k-th class. To convert these class scores into interpretable classification probabilities, the Softmax function is employed as the final layer, defined as

$$\text{Softmax}\left(y_i\right) = \frac{e^{y_i}}{\sum_{j=1}^{K} e^{y_j}} \,. \tag{5}$$

Here, y_i denotes the output value for the i-th class, K is the total number of classes, and e is the natural exponential constant. After Softmax normalization, the outputs are converted into probabilities ranging from 0 to 1, with their sum equal to 1, making them suitable for multiclass classification and effective for power capacitor state identification.

3. Modeling of Power Capacitor Defects and Measurement of Harmonic Current

3.1 Construction of defect models

In this study, seventy decommissioned 440 V/50 kVAR low-voltage power factor correction capacitors from Shihlin Electric & Engineering Co., Ltd. were examined to quantify capacitance degradation caused by long-term operation. LCR impedance measurements confirmed that all units exhibited notable capacitance reduction, indicating that prolonged service in distribution systems leads to measurable performance deterioration. To construct representative condition models, six capacitor states were defined: healthy, 20% degradation, 40% degradation, 60% degradation, 80% degradation, and failure. The healthy state was represented by new 45 μF capacitors, whereas the 20 and 40% degradation samples were obtained from capacitors subjected to controlled aging tests. Because consistent severely degraded samples are difficult to obtain from the field, the 60 and 80% degradation models were synthesized using equivalent series configurations: two 36 μF units in series for the 60% model and five 45 μF units in series for the 80% model. The failure class consisted of capacitors removed after actual electrical faults, which exhibited extreme damage and a residual capacitance of approximately 26 pF. Figure 1 shows the fabricated physical models of the capacitor defect conditions. The specifications of the power capacitors are listed in Table 1. These six categories form a comprehensive defect model covering the full range from healthy to failed conditions, providing a robust basis for analyzing how different degradation levels affect the performance and reliability of power capacitors.

3.2 Measurement architecture and preprocessing of charging harmonic currents

In this study, charging harmonic current measurements were conducted for the six constructed health states of power capacitors. The measurement setup employed a 110 V, 60 Hz mains supply, with each acquisition covering three fundamental cycles. A sampling window of 50 ms and a sampling rate of 20 MS/s were used, yielding a total of 1,000,000 data points to ensure the comprehensive capture of high-frequency transient features. Because the high-frequency charging currents generated during capacitor energization exhibit short durations, high frequencies, and relatively small amplitudes that are susceptible to electrical noise, appropriate signal conditioning is essential for accurately identifying their harmonic characteristics. To address this, an HFCT was utilized for primary current sensing, followed by a

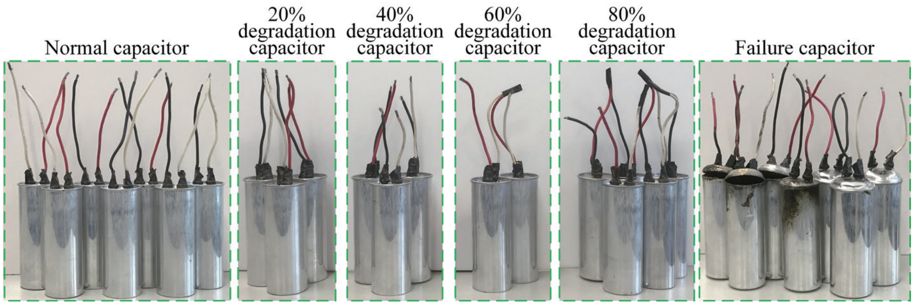

Fig. 1. (Color online) Power capacitor defect model.

Table 1
Specifications of low-voltage power factor correction capacitors.

Capacitor condition	Capacitance	Phase	Frequency (Hz)	Rated voltage (V)
Normal	45 μF	Single-phase	60	440
20% degradation	36 μF	Single-phase	60	440
40% degradation	27 μF	Single-phase	60	440
60% degradation	18 μF	Single-phase	60	440
80% degradation	9 μF	Single-phase	60	440
Failure	26 pF	Single-phase	60	440

high-pass filter to suppress low-frequency components and ambient noise. A non-inverting amplifier was further incorporated to enhance the amplitude of the high-frequency harmonic currents, thereby improving signal readability and measurement accuracy. The resulting conditioned current signals were acquired using a high-bandwidth oscilloscope and subsequently transferred to a computer via a universal serial bus interface for fault diagnosis and signal analysis. The experimental measurement circuitry and the capacitor charging harmonic current detection platform are illustrated in Figs. 2 and 3, respectively.

4. Experimental Results and Analysis

The fault diagnosis procedure proposed in this study is illustrated in Fig. 4, where the overall methodology is based on low-voltage AC withstand charging tests for signal acquisition and condition assessment. During measurement, an autotransformer is used to regulate the applied voltage across the two terminals of the capacitor under test, thereby establishing stable charging conditions and enabling the capture of its charging harmonic current response. The charging

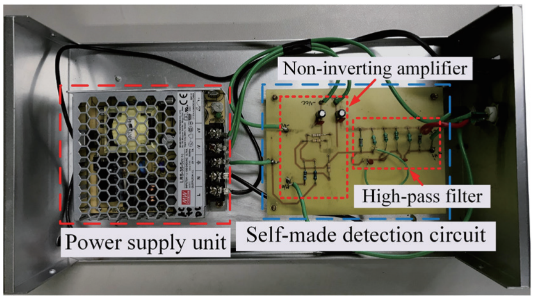

Fig. 2. (Color online) Self-made detection circuit.

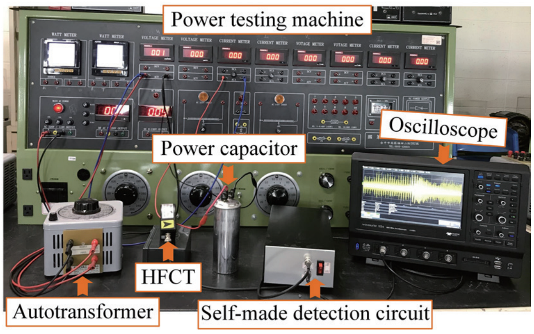

Fig. 3. (Color online) Power capacitor detection experimental platform.

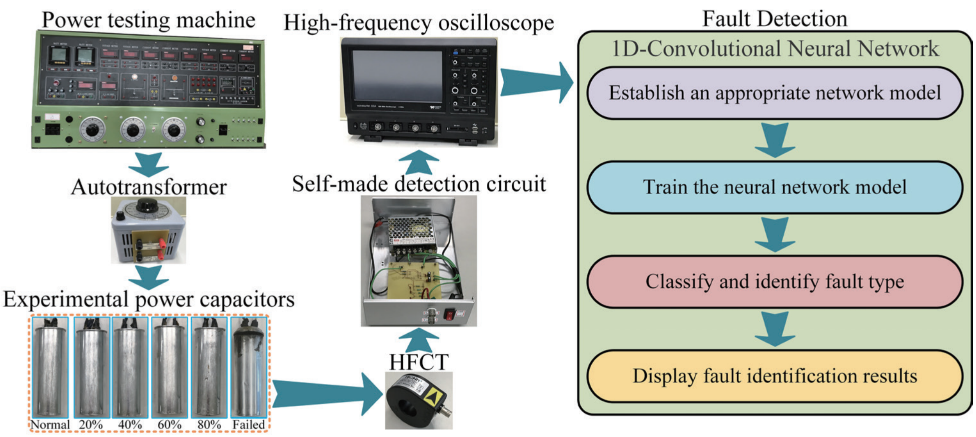

Fig. 4. (Color online) Flowchart of proposed power capacitor fault diagnosis system.

current is measured using an HFCT, and the acquired signal is subsequently processed through a custom-designed front-end circuit that performs high-pass filtering and amplification. The conditioned waveform is recorded by a high-bandwidth oscilloscope and utilized as the input data for the deep learning model. Unlike traditional approaches that depend on manual feature extraction and frequency-domain transformation, the proposed method directly feeds the raw time-domain current waveform into a 1D-CNN. Through convolution and pooling operations, the network automatically extracts representative features for classifying the degradation levels and fault conditions of power capacitors.

4.1 Measurement of actual signals

In this study, the six health conditions of power capacitors were analyzed, namely, the normal state, the failure state, and four degradation levels of capacitance decline. For each condition, real capacitor samples were tested to obtain their charging harmonic current signals, which were preprocessed using a high-pass filter and a non-inverting amplification circuit to ensure adequate signal quality. A total of 90 signal samples were collected for each category, of which 60 randomly selected samples were used for training the neural network model, whereas the remaining 30 samples were reserved for testing. The raw charging harmonic current waveforms corresponding to the normal capacitor, the four degradation levels (20–80%), and the failed capacitor are shown in Fig. 5.

4.2 Results and analysis of fault diagnosis

The proposed power capacitor fault diagnosis system was implemented in MATLAB 2025a, and the classification algorithm was tested and validated on a workstation equipped with an Intel® Core™ i7-12700 3.6-GHz processor, an NVIDIA GeForce RTX 4070 GPU, and a 64-bit Windows 11 Professional operating system. To perform multiclass identification of capacitor

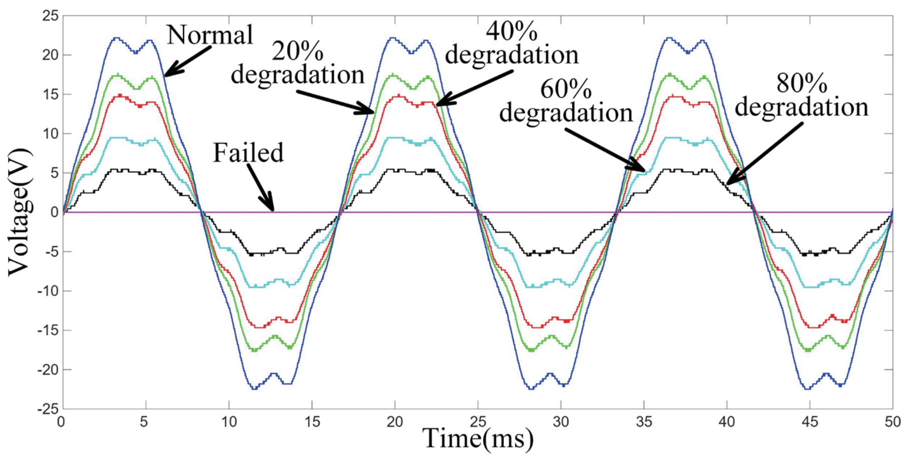

Fig. 5. (Color online) Original charging harmonic current waveforms of power capacitors.

conditions, a 1D-CNN was developed. The proposed network architecture comprises three convolutional layers, each configured with 16 filters and a kernel size of 3 applied along the temporal axis to effectively extract representative temporal features. These layers are sequentially integrated with three max-pooling layers, a flatten layer, and a final fully connected layer utilizing a Softmax classifier to facilitate robust multistate fault categorization. The overall structure of the designed 1D-CNN model is illustrated in Fig. 6.

A total of 540 charging harmonic current samples were collected from power capacitors in this study, among which 360 samples were used to train the 1D-CNN model for feature learning and classifier construction. Each of the six capacitor conditions was assigned 90 samples for training, whereas the remaining 180 non-overlapping samples were used as test data to evaluate the model's ability to identify different fault types. As summarized in Table 2, the proposed 1D-CNN-based diagnosis method achieves high accuracy across all capacitor states, yielding an overall classification accuracy of 97.78%. The classes corresponding to the healthy capacitor with 20% and 40% capacitance degradation exhibit comparatively lower accuracy (both 93.33%), primarily due to their highly similar charging harmonic current amplitudes, which reduces the separability of these two conditions. Nonetheless, all other categories—including the healthy, severely degraded, and failed capacitor states—achieve 100% precision, recall, and F1-score, confirming the robustness and reliability of the proposed approach. The classification outcomes are further illustrated in the confusion matrix shown in Fig. 7, where diagonal elements represent correct predictions and off-diagonal elements denote misclassifications.

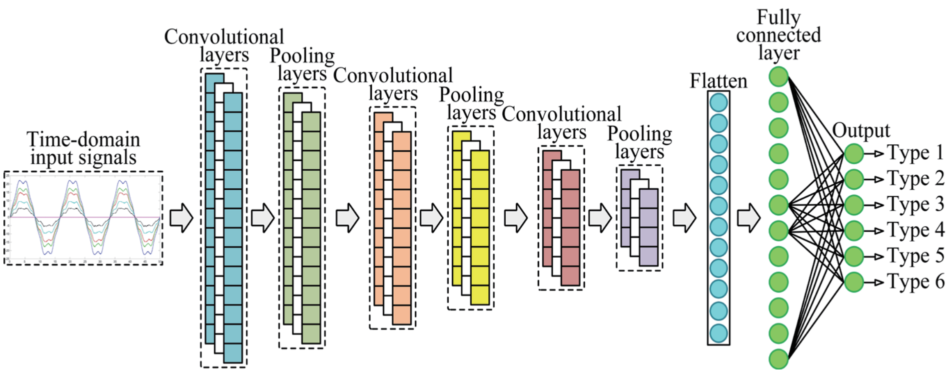

Fig. 6. (Color online) Architecture of proposed 1D-CNN model.

Table 2
Classification categories and diagnostic performance for power capacitor fault types.

Fault type	Precision (%)	Recall (%)	F1-score (%)	Accuracy (%)
Normal	100	100	100	97.78
20% degradation	93.33	93.33	93.33	
40% degradation	93.33	93.33	93.33	
60% degradation	100	100	100	
80% degradation	100	100	100	
Failure	100	100	100	

Class-wise accuracy metrics are displayed along the matrix margins, and the bottom-right entry provides the overall accuracy, demonstrating the effectiveness of the proposed diagnosis method.

4.3 Comparative analysis with other algorithms

To further validate the effectiveness of the proposed 1D-CNN-based method, a performance comparison was conducted using a 2D-CNN and an ENN as benchmark models. All classifiers were trained and tested using identical datasets, and each algorithm was executed five times independently; the average classification accuracy was reported to ensure the reliability of the results. As shown in Table 3, the 1D-CNN achieves the best performance, with all four metrics reaching 97.78%. Compared with the 2D-CNN and ENN, it demonstrates higher precision and recall, indicating more effective fault classification with reduced false alarms and missed detections. Although the ENN exhibited the shortest computation time, its classification performance was significantly lower than that of the 1D-CNN. Moreover, the 1D-CNN not only

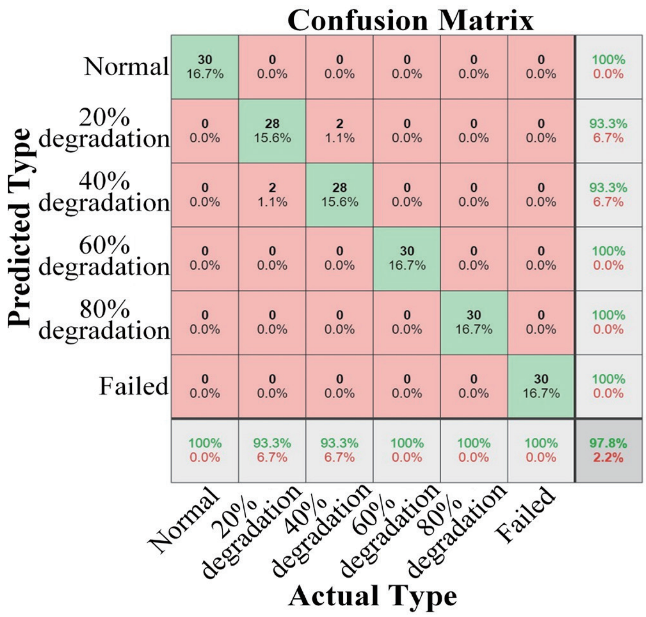

Fig. 7. (Color online) Confusion matrix of power capacitor fault diagnosis results.

Table 3
Results of different fault detection methods.

Algorithms	Accuracy (%)	Precision (%)	Recall (%)	F1-score (%)	Identification time (s)	Ranking
1D-CNN	97.78	97.78	97.78	97.78	0.22	1
2D-CNN	96.11	96.13	96.11	96.11	0.28	2
ENN	92.22	92.31	92.22	92.26	0.01	3

surpassed the 2D-CNN in accuracy but also required less computational time. This advantage is primarily attributed to the 1D-CNN's ability to directly process raw time-domain current signals, eliminating the need for image transformation or additional feature extraction that may introduce information loss. Overall, the results presented in Table 2 clearly demonstrate that the proposed 1D-CNN method provides the highest classification accuracy and superior overall performance for power capacitor fault diagnosis, highlighting its strong potential for practical implementation.

5. Conclusions

In this study, we proposed a power capacitor degradation and fault diagnosis method based on a 1D-CNN, in which high-frequency time-domain charging current signals obtained from a low-voltage AC withstand test were captured using a high-frequency current transformer and analyzed directly using the model for automated feature extraction. The developed system successfully identified six operating conditions, namely, healthy, four levels of capacitance degradation, and failure. Experimental results demonstrated that the proposed 1D-CNN achieved an overall classification accuracy of 97.78%, with 100% accuracy in both highly degraded and failed categories, outperforming the 2D-CNN and ENN benchmarks. These results confirmed that directly utilizing raw time-domain signals enhances both diagnostic efficiency and robustness. The main contributions of this work include establishing a quantifiable capacitor degradation model, developing a deep-learning diagnostic framework that requires no manual feature extraction, and validating the high feasibility of using time-domain current signals for capacitor fault identification. Future research may incorporate multichannel sensing or online monitoring data to further improve model generalization in practical environments and advance toward real-time monitoring and intelligent maintenance deployment.

References

1 H. M. Umran, F. Wang, and Y. He: IEEE Access **8** (2020) 40413. https://doi.org/10.1109/ACCESS.2020.2976526
2 L. C. Kien, T. T. Nguyen, T. M. Phan, and T. T. Nguyen: Sustainable Energy Technol. Assess. **52** (2022) 102253. https://doi.org/10.1016/j.seta.2022.102253
3 X. Gu, X. Mao, X. Shi, J. Zhou, X. Shen, J. Zhang, and J. Lu: J. Appl. Polym. Sci. **142** (2025) e57390. https://doi.org/10.1002/app.57390
4 S. Lu, H. Chai, A. Sahoo, and B. T. Phung: IEEE Trans. Dielectr. Electr. Insul. **27** (2020) 1861. https://doi.org/10.1109/TDEI.2020.009070
5 C. K. Chang and Y. H. Lin: IEEE Trans. Dielectr. Electr. Insul. **32** (2024) 1147. https://doi.org/10.1109/TDEI.2024.3431431
6 A. Ishaq, M. Junaid, G. Amjad Hussain, S. U. Khan, Y. Chen, and D. Yu: IEEE Trans. Instrum. Meas. **74** (2025) 1. https://doi.org/10.1109/TIM.2025.3562981
7 H. Zheng, Y Liang, J. Li, D. Yang, J. Jing, P. Li, J. Kang, and W. Liang: IEEE Trans. Power Delivery **40** (2025) 2533. https://doi.org/10.1109/TPWRD.2025.3584132
8 M. S. R. M. Saufi, M. F. Isham, M. H. A. Talib, and M. Z. M. Zain: J. Vib. Eng. Technol. **12** (2024) 5935. https://doi.org/10.1007/s42417-023-01228-5
9 Y. Gu, Y. Zhang, M. Yang, and C. Li: Appl. Sci. **13** (2023) 4192. https://doi.org/10.3390/app13074192
10 S. Rajagopalan, J. Singh, and A. Purohit: Proc. Inst. Mech. Eng., Part E: J. Process Mech. Eng. **10** (2024) 1177. https://doi.org/10.1177/09544089241235707
11 P. Chiradeja and A. Ngaopitakkul: IEEE Access **10** (2022) 86765. https://doi.org/10.1109/ACCESS.2022.3199362

12 S. Govindarajan, A. Morales, J. A. Ardila-Rey, and N. Purushothaman: Measurement **216** (2023) 112882 https://doi.org/10.1016/j.measurement.2023.112882
13 B. A. Siddiqui, P. Pakonen, and P. Verho: IEEE Trans. Dielectr. Electr. Insul. **24** (2017) 209. https://doi.org/10.1109/TDEI.2016.005908
14 S. Kaziz, M. H. Said, A. Imburgia, B. Maamer, D. Flandre, P. Romano, and F. Tounsi: Energies **16** (2023) 1978 https://doi.org/10.3390/en16041978
15 J. He, X. Li, Y. Chen, D. Chen, J. Guo, and Y. Zhou: Shock Vib. **2021** (2021) 6687331. https://doi.org/10.1155/2021/6687331
16 R. F. Ribeiro Junior, I. A. S. Areias, M. M. Campos, C. E. Teixeira, L. E. B. Silva, and G. F. Gomes: Measurement **190** (2022) 110759. https://doi.org/10.1016/j.measurement.2022.110759
17 Y. R. Choi and R. M. Kil: IEEE Trans. Image Process. **30** (2021) 1015. https://doi.org/10.1109/TIP.2020.3040847
18 S. Mantach, A. Lutfi, H. Moradi Tavasani, A. Ashraf, A. El-Hag, and B. Kordi: Energies **15** (2022) 5005. https://doi.org/10.3390/en15145005
19 Y. Li, Q. Yao, H. Yu, X. Xie, Z. Shi, S. Li, H. Qiu. C. Li. C. Li, and J. Qin: Front. Bioeng. Biotechnol. **10** (2022) 996723. https://doi.org/10.3389/fbioe.2022.996723
20 C. Rajesh, R. Sadam, and S. Kumar: Expert Syst. Appl. **239** (2024) 122509. https://doi.org/10.1016/j.eswa.2023.122509
21 A. Heinecke, J. Ho, and W. Hwang: IEEE Signal Process Lett. **27** (2020) 1175. https://doi.org/10.1109/LSP.2020.3005051
22 Z. Hu, J. Zhang, and Y. Ge: IEEE Access **9** (2021) 22371. https://doi.org/10.1109/ACCESS.2021.3054915

About the Authors

Hong-Wei Sian received his M.S. degree in electrical engineering from National Changhua University of Education (NCUE), Changhua City, Taiwan, in 2006, and his Ph.D. degree in electrical engineering from National Taiwan University of Science and Technology (NTUST), Taipei City, Taiwan, in 2024. He is currently an assistant professor in the Department of Electrical Engineering, National Chin-Yi University of Technology, Taichung City, Taiwan. His research interests include equipment fault diagnosis, renewable energy systems, programmable logic controllers, and automation control applications.
(hwsian@ncut.edu.tw)

Meng-Hui Wang received his M.S. and Ph.D. degrees in electrical engineering in 1990 and 1994, respectively, from National Taiwan University of Science and Technology. He joined National Chin-Yi University of Technology in August 1994 and is now affiliated with the Department of Electrical Engineering as a lifetime distinguished professor. His major areas of research include renewable energy systems, power systems, extension theory, and AI applications. He is a member of the Chinese Association of Artificial Intelligence, the vice president of the Taiwan Education Society of Innovation & Invention, and the chairman of the 6th Intelligent Living Technology Association of Taiwan. He was the general chair of the 1st Intelligent Living Technology Conference (2006) and the honorary co-chair of the 2012 International Symposium on Computer, Consumer, and Control.
(wangmh@ncut.edu.tw)

Chen-Hsiang Sun received his bachelor's degree from the Department of Electrical Engineering at National Chin-Yi University of Technology, Taichung City, Taiwan, in 2024, and is currently pursuing his master's degree in the same department. His main research interest is fault diagnosis.
(alexhsu9251@gmail.com)